SINGLE MODE SEMICONDUCTOR LASERS FOR LIDAR AND OTHER NASA APPLICATIONS

Interim or Final Report

JPL Task 1023

Kamjou Mansour, Section 384
Alexander Ksendzov, Section 346

A. OBJECTIVES

The challenge of making narrow-linewidth semiconductor lasers in the 2-μm region can be met with two distinct approaches. One is to emulate the communications industry, i.e. make distributed feedback (DFB) or Distributed Bragg Reflector (DBR) lasers. Making DFB or DBR lasers requires re-growth of semiconducting layers on top of an etched grating – a difficult process that has to be learned anew when shifting from communication wavelengths to the 2-μm region. On the other hand, the hybrid technique explored here requires only a simple Fabri-Perot gain medium. But there is a trade-off – the hybrid technique requires that the external feedback element is low-loss, has a mode profile close to that of the gain medium, and that the gain chip is precisely aligned to the external feedback element.

While we have previously demonstrated the technique to satisfy the latter requirement [1, 2], the ability to satisfy the first two requirements needs to be explored. In this work we have set out to demonstrate low-loss waveguides for external feedback, and to produce designs for external waveguides providing a good match to the mode profile of a gain chip.

B. PROGRESS AND RESULTS

Measurement of loss in waveguides

There are several well-known techniques for measuring the waveguide loss. One is to acquire an image of the scattered light from the waveguide in top view using a camera, and use it to determine the light extinction from the point of entrance toward the exit. This technique was rejected since there are no cameras sensitive enough in the 2-μm range.

Another technique, the so-called “cut off” method, is based on using a series of waveguides of different lengths. Measured transmittance of these waveguides is compared to elucidate the waveguide loss. In our case, the waveguide mode has an oblong shape which is difficult to emulate with a fiber or a microscope objective, so the coupling losses would dominate the transmittance measurements.

We chose to use the ring-resonator transmittance to measure the loss. Its main advantage is its relative insensitivity to the coupling efficiency. The schematic representation of the ring structure is shown in Figure 1. For the waveguide, we have used Si_xN_y core and SiO_2 cladding materials grown by PECVD. The waveguide fabrication is described in detail in Refs. 1 and 2.

It is well known that the spectral transmittance curves of a ring resonator can be used to measure losses. The difficulty in our case is the absence of a source with variable wavelength.

We have overcome this difficulty in the following way. The expression for the resonator transmittance is [3]:

$$I = I_0 \frac{(1-R)^2 A}{(1-RA)^2 + 4RA\sin^2(\delta/2)} \qquad (1)$$

where R is the fraction of energy left in the input waveguide after the crossover region, A is the waveguide loss per turn, and δ is the roundtrip phase change of the light wave.

The latter can be expressed as $\delta = 2\pi\lambda/L$, where λ is the wavelength of light and L is the length of the ring. When cast in this form, it is apparent that the transmittance spectrum can be measured either by scanning the wavelength or by varying the ring length. The latter can be accomplished by heating or cooling the ring-resonator chip. We assembled a setup that provided temperature control for the ring-resonator chip, as well as a means of coupling 2.05-μm radiation of a single-mode DFB laser in and out of the resonator. The result of a measurement is depicted in Figure 2.

To interpret these data, we have used the expression (1) to derive a 2-dimensional map of finesse and coupling as functions of loss in the ring and cross coupling. Such a map is shown in Figure 3. For single-tap rings, such as shown in Figure 1, there are two possible solutions for the contrast. Therefore the value of cross coupling and loss derived from the measurement carries an ambiguity. The two crosses in Figure 3 denote the two possible solutions. Note that both of these solutions correspond to losses of less than 2 dB/revolution. Given the ring geometry with 1-mm radius and 200-μm coupling regions, this translates to less than 2 dB/cm loss. We believe that some of the loss is due to the racetrack geometry of the ring, whereby the transition from the straight coupling region into the curve results in additional loss. Even if this is not the case, the loss is quite acceptable. We plan to use 3-mm-long gratings, so the round-trip loss will be only 1.2 dB.

Gain chip to external grating coupling

To facilitate the efficient coupling of light between the gain chip and the external grating element, the modes of the two components need to be similar. The one-dimensional coupling efficiency (we are concerned here solely with the mode shape) can be expressed as an overlap integral [4]:

$$\frac{\left|\int E_i E_g^* dx\right|}{\int |E_i|^2 dx \int |E_g|^2 dx} \qquad (2)$$

where E_i and E_g are the (field) mode profiles of the gain chip and the external waveguide respectively. The expression (2) should be used along both horizontal and vertical directions to find the total coupling efficiency. The general scheme is as follows: first, measure far-field profiles of the existing gain chips, find the dimensions of the Gaussian modes that produced them, and finally, design waveguides with good overlaps with the found modes. The assumption of Gaussian profiles for the gain-chip modes is somewhat arbitrary [4], but it makes the problem immediately tractable.

We have assembled the far-field measurement setup using two rotational stages. The detector was mounted on the arm that executes motion along true azimuthal and inclination

angles around the emitting facet of the gain chip. We have chosen this simple optical layout because, unlike other setups, it contains no curved optical surfaces and therefore does not depend on precise focusing or collimation alignment for precision measurement.

We have had two kinds of gain chips available: InGaAsP- and InGaSb-based devices. A 3-dimensional representation of the far-field intensity for the InGaAsP chip is shown in Figure 4.

To derive the mode size that generated such a far-field profile, we have fit the horizontal and vertical cross sections of these data to Gaussian line shapes. The 2-dimensional data and the fit results are shown in Figures 5 and 6. The parameter *w* represents the width of the profiles in degrees. The corresponding width d_m of the (Gaussian) gain chip mode is found using the following relationship:

$$d_m = \frac{2}{k\tan(w)}, \qquad (3)$$

where k is the wavevector of light, and *w* is the angular divergence of the beam. In Table 1, we summarize the measurements of the mode profiles for the existing gain chips.

Table 1. Measured mode sizes for existing gain chips and overlap integrals with the "best design" external waveguide.

	InGaAsP		InGaSb	
	vert. section	hor. section	vert. section	hor. section
measured d_m	1.18 μm	2.36 μm	0.56 μm	3.8 μm
overlap with external waveguide	0.92	0.92	0.9	0.62
overlap x*y	0.84		0.56	

Using these data, we started to design the waveguides, using materials available to us at the Microdevices Laboratory at JPL. In order to reproduce the high vertical divergence, we used the SixNy/SiO2 combination, since it provides the highest index contrast between the core and the cladding. The waveguide cross section is shown in Figure 7. The refractive indexes were obtained using spectroscopic ellipsometry.

The highest vertical divergence was achieved at h=0.28 μm. This provided the overlap with the vertical mode profile of InGaAsP gain chip of 0.92. The best fit to the horizontal mode profile was achieved for the ridge width of 2.5 μm and the etch depth d of 0.13 μm resulting in an overlap of 0.92. A better match was precluded by the appearance of the second mode. The total overlap was 0.84, corresponding to a 1.75-dB roundtrip loss at the interface. The best fit achieved for the InGaSb chip was 5 dB roundtrip. The results are summarized in Table 1.

C. SIGNIFICANCE OF RESULTS

To prove the feasibility of the hybrid approach to 2-μm narrow-linewidth lasers, we have studied the optical loss in Si_xN_y/SiO_2 PECVD waveguides and designed waveguides exhibiting

good overlaps with the existing gain chips. We found that the optical loss in our waveguides is less than 2 dB/cm, while the roundtrip coupling loss at the interface with the gain chip can be as low as 1.75 dB. Using a 3-mm-long external grating, we can achieve a total 2.95-dB roundtrip loss. This compares favorably with conventional DBR lasers [5] and proves viability of the hybrid approach to fabricating narrow-linewidth lasers in the 2-μm spectral range.

D. FINANCIAL STATUS

The total funding for this task was $98,000 all of which has been expended.

E. PERSONNEL

No other personnel were involved.

F. PUBLICATIONS

None.

G. REFERENCES

[1] A. Ksendzov, K. Mansour. "Hybrid fabrication of single frequency semiconductor lasers", Electronics Letters **38** pp. 1536-1537 (2002)

[2] A. Ksendzov, K. Mansour. "Hybrid single mode lasers fabricated using Si/SiO2/SiON micromachined platforms", SPIE paper **4987**-24 (2003).

[3] D. Rafizadeh, J.P Zang, R.C Tiberio, and S.T. Ho. "Propagation loss measurements in semiconductor microcavity ring and disk resonators", Journ. of Lightwave Technology **16** (7) pp. 1308-1314 (1998)

[4] K.Y. Lee, W.-S. Wang. "Non-Gaussian beams in direct coupling from laser diodes into optical waveguides via small gaps", Microwave and Opt. Technol. Lett., **5** pp. 99-101 (1992).

[5] "Diode lasers and photonic integrated circuits" by L.A. Couldrin, S.W. Corzine (J. Wiley & Sons, NY 1995).

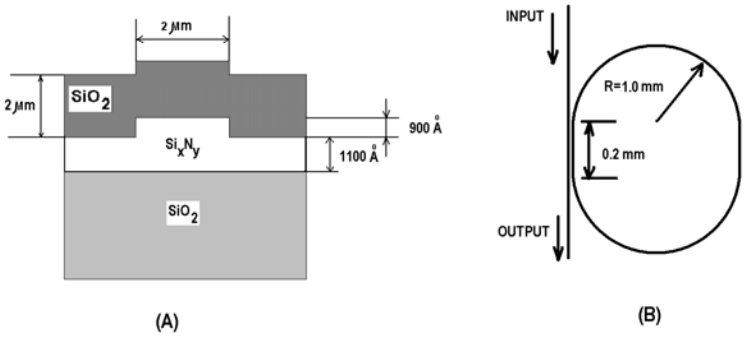

Figure 1. (A) The waveguide cross section. (B) The ring resonator layout. The racetrack shape was necessary to facilitate strong (0.1 or more) coupling between the straight waveguide and the ring.

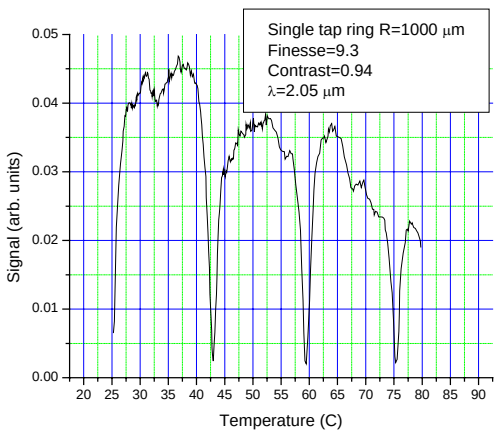

Figure 2. Measurement of loss in a ring resonator. The finesse and contrast parameters are shown in the insert.

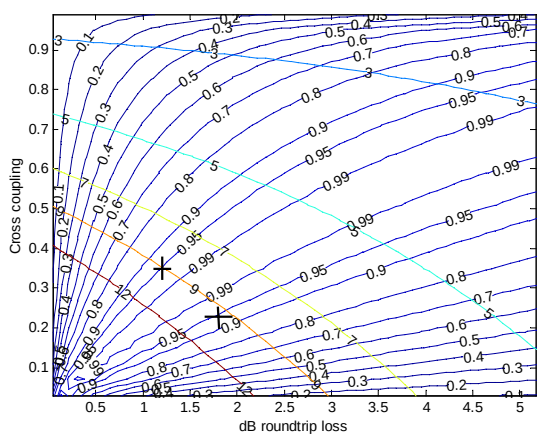

Figure 3. Two-dimensional map of finesse ("horizontal" lines) and contrast (lines converging toward the origin) vs. loss and coupling. Crosses mark the two possible solutions for the ring measurement pictured in Fig. 2. Both solutions correspond to better than 2 dB/cm loss (see text).

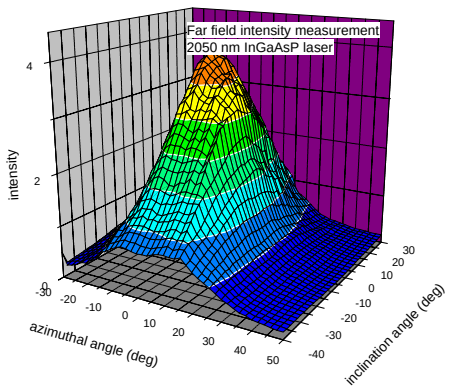

Figure 4. Three-dimensional representation of the far-field intensity recorded from InGaAsP-based gain chip.

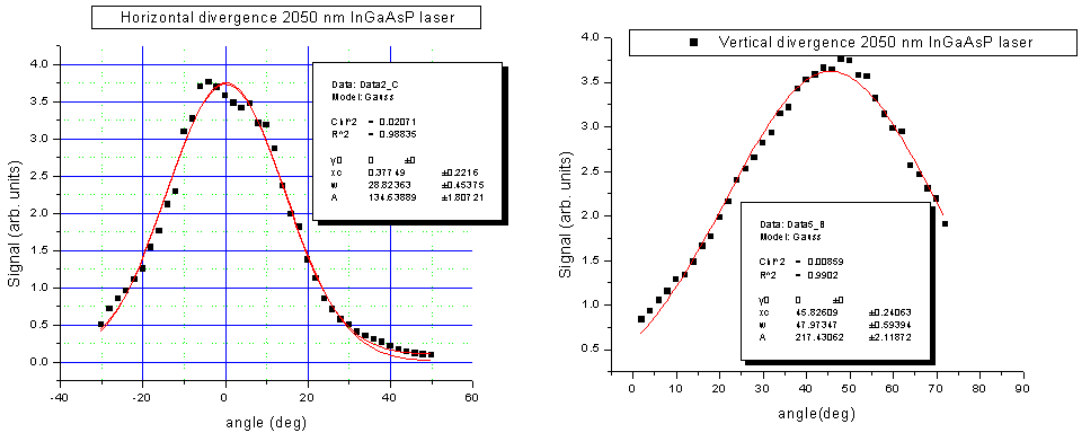

Figure 5. Horizontal and vertical cross sections of the far-field intensity recorded from InGaAsP-based gain chip.

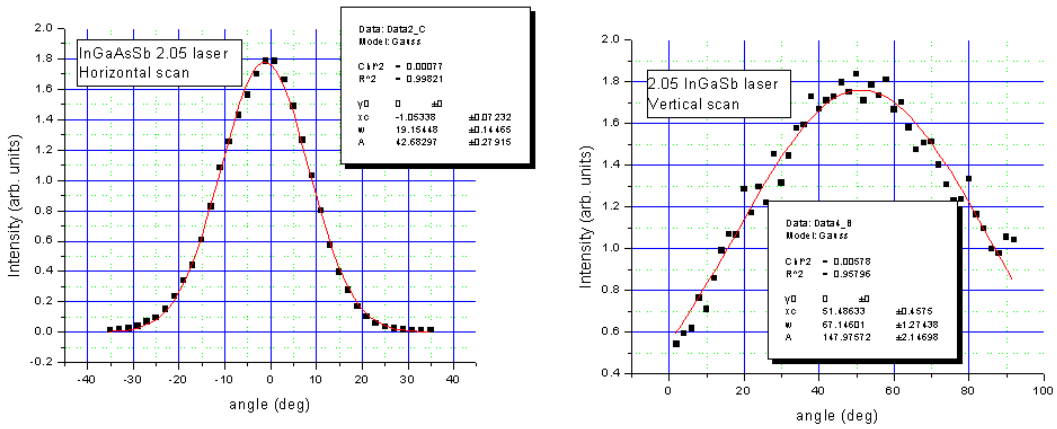

Figure 6. Horizontal and vertical cross sections of far-field intensity recorded from InGaSb-based gain chip.

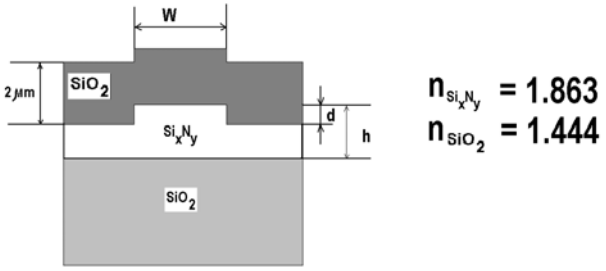

Figure 7. The external feedback element waveguide profile.